

Tension-compression strength asymmetry of nanocrystalline α -Fe₂O₃+fcc-Al ceramic-metal composites

Vikas Tomar^{a)}

Department of Aerospace and Mechanical Engineering, University of Notre Dame, Notre Dame, Indiana 46556

Min Zhou^{b)}

George W. Woodruff School of Mechanical Engineering, Georgia Institute of Technology, Atlanta, Georgia 30332

(Received 17 April 2006; accepted 27 April 2006; published online 6 June 2006)

The dependence on composition and loading direction of the strength of nanocrystalline α -Fe₂O₃+fcc-Al composites is analyzed using molecular dynamics simulations with a recently developed multicomponent interatomic potential. Compressive strength values are found to be higher than the tensile strength values at all volume fractions of the phases. Reverse Hall-Petch relations are observed for tension and forward Hall-Petch relations are observed for compression. The observed asymmetry in behavior and the direct or reverse nature of the Hall-Petch relations are found to reflect the different manners in which pairwise electrostatic forces influence grain boundary sliding which is the primary deformation mechanism. © 2006 American Institute of Physics. [DOI: 10.1063/1.2210797]

At the macroscopic scale, polycrystalline materials often show asymmetries in tensile and compressive strength values due to differences in mechanisms of defect nucleation and propagation under tensile and compressive loadings, see, e.g., Jiao *et al.*¹ At the nanoscale, tension-compression asymmetry can arise for other reasons. For instance, Diao *et al.*² reported that the yield strength of Au nanowires is asymmetric because of significant surface-stress-induced internal stresses. Recently, Lund *et al.*³ observed a tension-compression asymmetry in the deformation of nanocrystalline Ni with nanometer grain sizes which is attributed to disordered atomic structures in grain boundaries (GBs). Here, we analyze this underlying mechanism that gives rise to the asymmetry in tensile and compressive strengths of nanocrystalline α -Fe₂O₃+fcc-Al composites and how this asymmetry is affected by the volume fractions of the phases. For this purpose, molecular dynamics (MD) simulations are performed at 300 K. The interatomic potential used consists of a functional form that allows multibody, pairwise, and electrostatic interactions among different species in the system to be described, cf. Tomar and Zhou,⁴ Tomar,⁵ and Tomar and Zhou.⁶

Figure 1 shows the nanocrystalline structures with different volume fractions of the phases and different average grain sizes analyzed (labels on the structures are used for identification purposes). Three average grain sizes are involved: (1) 8 grains with an average grain size of 7.2 nm; (2) 27 grains with an average grain size of 4.7 nm; and (3) 64 grains with an average grain size of 3.9 nm. A combination of the well-established Voronoi tessellation method and the inverse Monte Carlo method is used to ensure that the grain sizes conform to prescribed log-normal distributions with a 10% standard deviation, see Ref. 5. For comparison purposes, nanostructures of different compositions at each grain

size have the same grain morphologies and the same grain orientation distribution. The constituent volume fractions are specified using a random number generator. The orientations of the grains are specified by choosing the [001], [010], or [011] crystalline axis of each grain using another random number generator. The model is implemented in a modified version of the scalable parallel MD code DL_POLY 2.14 (Smith *et al.*⁷).

To effect displacement-controlled quasistatic uniaxial deformation, a combination of the algorithms for *NPT* and *NVT* ensembles is used. The combined algorithm consists of alternating steps of stretching and equilibration to approximate quasistatic deformation. The application of the algorithm results in conditions of uniaxial strain. During equi-

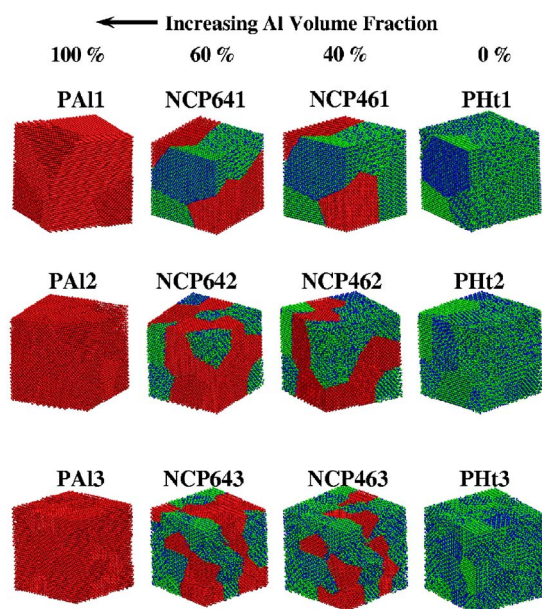


FIG. 1. (Color online) Nanocrystalline structures in with different Al volume fractions and grain sizes of (a) 7.2, (b) 4.7, and (c) 3.9 nm.

^{a)} Author to whom correspondence should be addressed; electronic mail: vikas.tomar@nd.edu

^{b)} Electronic mail: min.zhou@gatech.edu

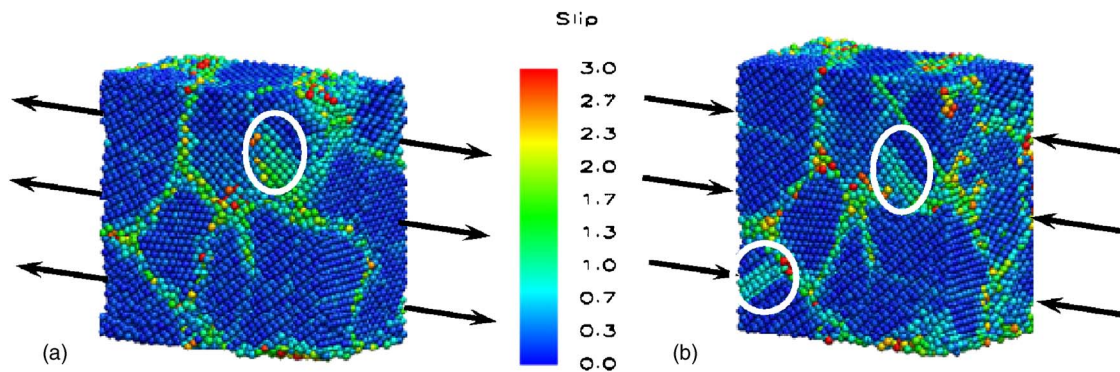


FIG. 2. (Color online) Deformed configurations of nanocrystalline Al with grain size 4.7 nm at strain levels corresponding to the calculation of flow strength values (a) in tension and (b) in compression.

bration, *NVT* equations of motion are used. During stretching, the computational cell is stretched in the loading direction using the NPT equations of motion of Melchionna *et al.*⁸ Based on the convergence of stress-strain relations for different equilibration periods, a stretch increment of 0.05 ps and an equilibration period of 2.0 ps following each load step are chosen and used. For this combination, fluctuations in the stress values are within $\pm 5\%$ of the mean stress at all strain levels. To approximate three-dimensional (3D) bulk behavior, periodic boundary conditions (PBCs) are applied in all directions of the simulation cell. The discussion here focuses on the flow stress beyond initial yielding. This strength measure is calculated as the average stress in the region of the stress-strain curve where the stress reaches a maximum, see, e.g., Schiøtz *et al.*⁹ and Schiøtz and Jacobsen¹⁰ also calculated the flow stress by averaging the stress values at three arbitrary points in the strain interval of 7%–10%.

Figure 2 shows the deformed configurations of the pure Al structure with a grain size of 4.7 nm at a tensile strain of 7.5% [Fig. 2(a)] and a compressive strain of 15% [Fig. 2(b)]. These are the configurations at which the maximum tensile and compressive stresses are observed, respectively. The atoms are colored using the slip-vector approach of Kelchner *et al.*¹¹ to identify the formation of dislocations and other defects. In both tension and compression, stacking fault formation (see circles) and motion of atoms along GBs (defined as consisting of atoms with slip-vector magnitudes greater than 0.3 in the figure) are active deformation mechanisms. However, the dominant mechanism is GB sliding and dislocation motion inside grains plays only a minor role. Most

importantly, atoms in the GBs move in different manners during tension and compression, as pointed out by Lund *et al.*³ The primary reason for this difference is the disordered atomic arrangements in GBs. Specifically, in an ordered lattice, the neighbors of an atom are placed symmetrically after small deformations in tension and compression. In addition, the magnitude of the net force experienced by an atom from its neighbors is the same for small deformations in tension and compression. In GBs, however, the displacements of atoms are not symmetric in tension and compression and the asymmetry increases as deformation progresses due to the nonlinear nature of interatomic interactions. In addition, the number of atomic neighbors within a cutoff radius for a GB atom can be different in tension and compression and changes as deformation evolves. Consequently, the force experienced by a GB atom during compression is different from that in tension, leading to different deformation behaviors. Even the minor effects of dislocations on deformation are asymmetric in tension and compression. In particular, note that in Fig. 2, stacking faults are formed in different grains for tension and compression. The same deformation mechanisms are operative for the other structures in Fig. 1 as well.

Figure 3 shows the flow strengths for tension [Fig. 3(a)] and compression [Fig. 3(b)] as functions of average grain size. The strengths under compression are higher than those for tension. This is consistent with the observed differences in the deformation mechanism. Note that the interatomic force between two atoms increases faster under compression than under tension, leading to higher stresses in compression

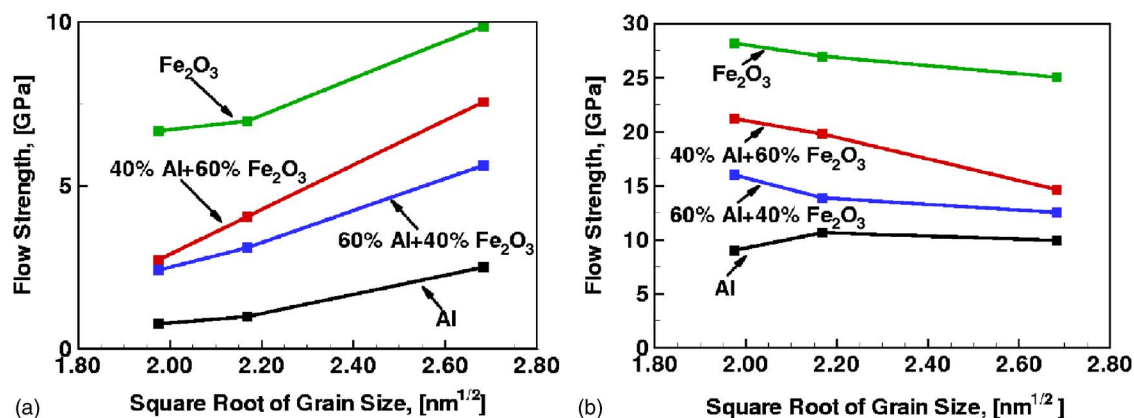


FIG. 3. (Color online) An examination of the dependence of the flow strength on the variation in square root of the grain size in all the nanocrystalline structures during (a) tensile deformation and (b) compressive deformation.

for the same amount of deformation (or atomic displacements). The disorder in GB atomic structures further accentuates this difference, cf. Lund *et al.*³ There is also an asymmetry in the strain levels achieved in tension and compression, cf. Tomar.⁵ In tension, the maximum stress occurs at smaller strains ($\sim 7\% - 10\%$). In compression, the maximum stress occurs at strains between $10\% - 15\%$.

For nanocrystalline Al reverse Hall-Petch (HP) relations in both tension and compression are observed. Since dislocation activities are negligible here, the softening seen as the average grain size is decreased is attributed to the sliding of grains along GBs and the increase in the fraction of GB atoms as the grain size is reduced. The relations in Fig. 3 show nonlinearity. The orientation mismatch (high angle versus low angle) between neighboring grains at GBs plays an important role in determining the deformation mechanism. This factor contributes to the nonlinearity of the HP relations in Fig. 3. A similar trend has been reported by Schiøtz *et al.*¹² for nanocrystalline Cu (MD simulations), by Lund *et al.*³ for nanocrystalline Ni (MD simulations), and by El-Sherik *et al.*¹³ for electroplated Ni (experiments).

In Fig. 3(a), there is an increase in the slope of the HP relationship with an increase in the volume fraction of the Fe_2O_3 phase. Increase in the HP slope with increase in the volume fraction of the Fe_2O_3 phase implies increased weakening of the nanocrystalline structures with reduction in the average grain size. Fe_2O_3 is a ceramic with mixed ionic-covalent bonds. Accordingly, composites with the Fe_2O_3 phase have pairwise electrostatic interactions due to the presence of Fe^{3+} and O^{2-} ions. In addition, positively charged Al ions are present at the Al- Fe_2O_3 interfaces because of reduction of Fe_2O_3 by Al at the interface. As the volume fraction of the Fe_2O_3 phase increases, the electrostatic energy of the system increases. These electrostatic interactions are absent in the pure Al structures. Consequently, it can be concluded that the increases in the slope for the composites is due to the increases in the electrostatic energy of the structures. This observation implies that electrostatic forces that are tensile in nature enhances GB sliding which is the primary mechanism responsible for the decreases in strength as the average grain size is decreased.

For all the structures except nanocrystalline Al the reverse HP relationship during tension and the direct HP relationships during compression are observed. Tensile electrostatic forces cause an increase in the GB sliding resulting in increased slope of reverse HP relationships with increasing Fe_2O_3 phase volume fraction during tension. The same forces oppose GB sliding during compression attributable to the pairwise nature of the electrostatic forces. For a composite structure with a given Fe_2O_3 phase volume fraction, there is an increase in the electrostatic energy with reduction in the

grain size. Primary factor responsible is an increase in the Al- Fe_2O_3 interfaces which in turn cause an increase in positively charged Al ions. Coupled increase in the electrostatic forces effectively negates the effect of GB sliding causing an increase in strength with reduction in the grain size. Both the reverse and the direct HP relations are strongly dependent on composition. Structures with higher volume fractions of the Fe_2O_3 phase have higher strength values. This is expected since Fe_2O_3 is stronger than Al.

In general, the HP relations for the composite structures cannot be obtained from the relations for PAI (pure Al) and PHt (pure Fe_2O_3) through the rule of mixture based on the volume fractions of the Al and Fe_2O_3 phases, in contrast to what is known at higher size scales. The flow strength values in tension of composites with the relatively large average grain size of 7.2 nm can be obtained from the strengths of the pure phases using the rule of mixture. This, however, is not the case for the structures with average grain sizes of 4.7 and 3.9 nm due to the enhanced roles of GBs. This is because the deformation mechanisms in the nanocomposites are strongly affected by the Al- Fe_2O_3 interfaces. The relative orientation of the two phases at an interface significantly affects the contribution of the interface to the strength of a composite. Specifically, the higher interface-to-volume ratios at smaller grain sizes cause higher fractions of atoms to be associated with interfaces instead of grain interiors, resulting in stronger roles of interfaces at smaller grain sizes.

Support from an AFOSR MURI on Multifunctional Energetic Materials at Georgia Tech is gratefully acknowledged. Computations are carried out at the NAVO, ERDC, and AHPCRC MSRCs. The authors thank Professor Julian Gale for providing the molecular statics code GULP 1.3 and Professor Will Smith for providing DL_POLY2.14 which are modified and used in this research.

¹F. Jiao, D. Bettge, W. Osterle, and J. Ziebs, *Acta Mater.* **44**, 3933 (1996).

²J. Diao, K. Gall, and P. Dunn, *Nano Lett.* **4**, 1863 (2004).

³A. C. Lund, T. G. Nieh, and C. A. Schuh, *Phys. Rev. B* **69**, 012101 (2004).

⁴V. Tomar and M. Zhou, *Mater. Res. Soc. Symp. Proc.* **821**, 319 (2004).

⁵V. Tomar, Ph.D. dissertation, Georgia Institute of Technology, 2005.

⁶V. Tomar and M. Zhou, *Phys. Rev. B* (to be published).

⁷W. Smith, C. W. Yong, and P. M. Rodger, *Mol. Simul.* **28**, 385 (2002).

⁸S. Melchionna, G. Ciccotti, and B. L. Holian, *Mol. Phys.* **78**, 533 (1993).

⁹J. Schiøtz, T. Vegge, F. D. Di Tolla, and K. W. Jacobsen, *Phys. Rev. B* **60**, 11971 (1999).

¹⁰J. Schiøtz and K. W. Jacobsen, *Science* **301**, 1357 (2003).

¹¹C. L. Kelchner, S. J. Plimpton, and J. C. Hamilton, *Phys. Rev. B* **58**, 11085 (1998).

¹²J. Schiøtz, F. D. Di Tolla, and K. W. Jacobsen, *Nature (London)* **391**, 561 (1998).

¹³A. M. El-Sherik, U. Erb, G. Palumbo, and K. T. Aust, *Scr. Metall. Mater.* **27**, 1185 (1992).